DEVELOPMENT OF NOVEL GEOPHYSICAL–GEOTECHNICAL RELATIONSHIPS OF GRANITIC ENVIRONMENTS IN PENANG ISLAND, MALAYSIA

AKINGBOYE ADEDIBU SUNNY

UNIVERSITI SAINS MALAYSIA

2023

DEVELOPMENT OF NOVEL GEOPHYSICAL–GEOTECHNICAL RELATIONSHIPS OF GRANITIC ENVIRONMENTS IN PENANG ISLAND, MALAYSIA

by

AKINGBOYE ADEDIBU SUNNY

Thesis submitted in fulfillment of the requirements
for the degree of
Doctor of Philosophy

August 2023

ACKNOWLEDGEMENT

First and foremost, my deepest gratitude goes to God Almighty for His goodness, grace, and unfathomable mercy in my life. I need to exceedingly appreciate God Almighty for the quick success I have made in my Ph.D. program. I believe He will keep making me stronger, wiser, and more prosperous every day. I will continue to worship and thank Him for His never-ending wonders because I am nothing without Him.

My supervisor, P.Geol. Dr. Andy Anderson Bery, has my undying gratitude for his unwavering support, unrelenting efforts, and enormous contributions that made me complete the Ph.D. program on time with remarkable milestone success and achievements. Despite his busy schedule, he is constantly available both online and in person to handle any pressing research issues and related academic matters. His vast knowledge and dedication to his profession served as a springboard and source of inspiration for the intriguing scientific studies conducted under his supervision. His financial support for carrying out scientific projects is also appreciated.

Furthermore, the entire Geophysics Laboratory Staff (Messrs Azmi Abdullah, Zulkeflee Ismail, and Shahil Ahmad Kosaini), and all the undergraduate and M.Sc. students under my Supervisor at the School of Physics, Universiti Sains Malaysia, are thanked for their help during the research field data acquisition. Additionally, the School of Physics, Universiti Sains Malaysia, and the Geophysics departmental staff are highly appreciated for providing the required research facilities and a conducive learning environment. The academic staff and colleagues at the Department of Earth Sciences, Adekunle Ajasin University, are also appreciated for their steadfast support.

I sincerely appreciate my parents (Mr. Smart A. Akingboye and Mrs. C.N. Akingboye) for their immense prayers, financial support, and careful guidance to accomplish my goals and deepest dreams. I have come this far because of their eternal and unrivaled love. I ask God to spare their lives so they can enjoy the rewards of their labor. In addition, I want to thank all my loving siblings for their immeasurable prayers and kind wishes. I also appreciate my concerned relatives. To all my friends, Messers J.O. Fatokimi, O. Akinkuowo, G.N. Sambo, Akinnawo, Nofiu, and Dr. A.O. Ige, as well as Miss. Aziela and Atinuke J. Adegboyega, among others. I thank you for your general support, prayers, and heartfelt wishes always. Mr. G.N. Sambo is appreciated for assisting during the field data acquisition.

Most importantly, my appreciation goes to my cherished wife and adorable son, whose patience and endurance have allowed me to pursue my dreams in this country of vast opportunities. I know the significant dedication and sacrifices they have made for this program to be a success. I thank them for their unconditional love, trust, and faith. God bless you!

I am grateful to the Tertiary Education Trust Fund, Nigeria, for awarding the Ph.D. scholarship for this program. The prestigious Adekunle Ajasin University, my employer, is greatly acknowledged for granting me study leave and providing additional funding to undertake the doctorate program. The Short Research Stay Grant awarded by the Helmholtz Centre Potsdam – GFZ German Research Centre for Geosciences in Germany, under Dr. Hui Tang (Host Supervisor) is also acknowledged.

On a final note, I dedicate this thesis to God Almighty, My Late Father (Mr. Marcus A. Akingboye), my loving family, and the benefits of humanity.

Thanks, and God bless you ALL for your support and endless kind wishes!

TABLE OF CONTENTS

ACKNOWLEDGEMENT ..... **ii**

TABLE OF CONTENTS ..... **iv**

LIST OF TABLES ..... **viii**

LIST OF FIGURES ..... **x**

LIST OF SYMBOLS ..... **xv**

LIST OF ABBREVIATIONS ..... **xviii**

LIST OF APPENDICES ..... **xx**

ABSTRAK ..... **xxii**

ABSTRACT ..... **xxiv**

CHAPTER 1 INTRODUCTION **1**

1.1 Background 1

1.2 Problem Statement 7

1.3 Research Justification 9

1.4 Research Objectives 11

1.5 Research Questions 11

1.6 Scope of the Study 12

1.7 Motivation of the Study 13

1.8 Thesis Layout 14

CHAPTER 2 LITERATURE REVIEW **16**

2.1 Introduction 16

2.2 An Overview of Electrical Resistivity Methods 16

2.2.1 Theories and Principles of Electrical Resistivity Methods 17

2.2.2 Configurations, Sensitivities, and Performance of Electrode Arrays 21

2.3 Insights into Seismic Refraction Tomography 26

2.4 Review of Previous Works 30

2.4.1 ERT and SRT in Surficial and Subsurface Crustal Investigations 30

2.4.2 Soil-Rock Conditions and Quality (RQD and SPT N-values) 34

2.4.3 Velocity–Resistivity Statistical Relationships for Lithologic Units 41

2.5 Chapter Summary 53

CHAPTER 3 METHODOLOGY 54

3.1 Introduction 54

3.2 Geography of Penang Island 54

3.3 Regional Geology of Peninsular Malaysia 56

3.4 Geological Settings of Penang Island 59

3.5 Experimental Setups, Framework, and Flowcharts for the Research 61

3.5.1 Survey Geometry 64

3.5.2 Geophysical Field Surveys at Site Locations 67

3.5.2(a) Soil-Rock Characterization and Electrode Assessment at Site 1 68

3.5.2(b) Soil-Rock Characterization and Quality at Site 2 69

3.5.2(c) Soil-Rock Characterization and Quality at Site 3 71

3.5.3 Geophysical Field Data Acquisition for the Research 71

3.5.3(a) ERT Data Acquisition Procedures 71

3.5.3(b) SRT Data Acquisition Procedures 74

3.5.4 Geophysical Field Data Processing, Inversion, and Modeling for the Research 76

3.5.4(a) ERT Field Data Processing and Inversion 76

3.5.4(b) SRT Field Data Processing and Inversion 79

3.5.5 Rock Mass Quality Evaluation in the Study Area 81

3.5.6 Velocity-Resistivity Statistical Formulation and Development 84

3.5.7 Velocity-Resistivity Regression Analytical Modeling and Accuracy Assessment 86

3.6 Chapter Summary 89

CHAPTER 4 RESULTS AND DISCUSSION 90

4.1 Introduction 90

4.2 Results of Soil-Rock Variability Conditions and Architecture 90

4.2.1 Lithological Logs from Existing and New Boreholes in the Study Area 91

4.2.2 Subsurface Resistivity and Velocity Characterization 92

4.3 Discussion of Results 99

4.3.1 Spatial Variability of Surficial and Subsurface Soil-Rock Conditions in the Study Area 100

4.3.1(a) Soil-Rock Conditions and Architecture of Site 1 100

4.3.1(b) Soil-Rock Conditions and Architecture of Site 2 103

4.3.1(c) Soil-Rock Conditions and Architecture of Site 3 105

4.3.2 Characteristics and RMQ of Lithologic Units beneath the Study Area 111

4.3.2(a) RMQ: Velocity and RQD Relationships and Statistical Modeling 113

4.3.2(b) RMQ: Resistivity and RQD Relationships and Statistical Modeling 119

4.3.2(c) Correlation Between Measured (Borehole-Based) and Estimated RQD Values for Selected Data 122

4.3.2(d) Statistical Analysis of Velocity-Resistivity Models and N-value Models 126

4.3.3 Development of Velocity-Resistivity Statistical Relationships ... 132

4.3.3(a) SLR of the Observed and Logarithm Velocity-Resistivity Models 138

4.3.3(b) Velocity-Resistivity Relationships for Specific Lithologic Units 139

4.3.3(c) Accuracy of Velocity-Resistivity Relations and Predictive Modeling 142

4.3.4 Environmental Applicability of Velocity-Resistivity, RMQ, and Statistical Modeling of Soil-Rock Conditions in the Study Area 147

4.4 Novelty of the Research and Contribution to Existing Knowledge 150

4.5 Limitations of the Research 151

4.6 Chapter Summary 152

CHAPTER 5 CONCLUSION AND FUTURE RECOMMENDATIONS 153

5.1 Conclusion 153

5.2 Recommendations for Future Research 155

REFERENCES 156

APPENDICES

LIST OF PUBLICATIONS

LIST OF TABLES

Page

Table 2.1 A comprehensive summary of the electrical resistivity values for some earth materials in different localities. 21

Table 3.1 Studied sites with their coordinates and borehole lithological logs. 66

Table 3.2 Summary of the surveying parameters employed for the field data acquisition in the study area. 67

Table 4.1 Summary of the surficial to subsurface ρ and Vp models correlated with borehole-derived lithologic units in the study area. 110

Table 4.2 A comprehensive interpretation of the SLR plot for predicting RMQ from the RQD and Vp data of the near-surface lithologic units at Site 2. 114

Table 4.3 Comprehensive summary of SLR analysis to evaluate the RMQ of subsurface lithologic units at Site 2 in the study area. 117

Table 4.4 A comprehensive interpretation of the SLR plot for predicting RMQ from the RQD and ρ data of the near-surface lithologic units at Site 2.....121

Table 4.5 Correlation between the measured (borehole-based) and estimated (SRT- and resistivity-based) RQD values for selected datasets based on appropriate empirical relations.....123

Table 4.6 Summarized interpretation of the soil-rock quality of the study area. 126

Table 4.7 Ranges of SPT N-values for different soil conditions. 129

Table 4.8 Proposed range of SPT N-values for soil conditions in relation to their corresponding velocity values for tropical granitic terrains. ...129

Table 4.9 MLR results of the N-values with their corresponding average Vp and ρ values for the study area.....131

Table 4.10 Interpretation of the velocity-resistivity SLR model for the study area. 134

Table 4.11 A comprehensive SLR analysis of the filtered resistivity-velocity data for Binjai, Batu Maung, Penang Island. 137

Table 4.12 Summary of the velocity-resistivity SLR for each lithologic unit. ..141

Table 4.13 Correlation analysis between the measured and predicted velocity values for selected datasets from BH1 to BH6 at Site 2 based on appropriate velocity-resistivity empirical relationships. 143

Table 4.14 Interpretive summary of the modeled soil-rock profiles based on velocity-resistivity relationships and their suitability for infrastructure design in the study area. 147

LIST OF FIGURES

Page

Figure 2.1 (a) A single-point source electrode with electric flow current in the subsurface. (b) A schematic fundamental diagram of a four-electrode resistivity measurement at the earth's surface and the subsurface distribution of the generated current flow. 18

Figure 2.2 Resistivity chart for the range of values for rocks, soils, and minerals. 20

Figure 2.3 Array types with their respective geometric configurations of the electrode's quadrupole and geometric factors 24

Figure 2.4 (a) Schematic diagram of a simple two-layered travel time curves model. (b) A typical seismic acquisition diagram of a simple two-layered model showing the direct, reflected, and refracted seismic waves from a source (S) to a surface geophone detector (D). 27

Figure 3.1 Google location of map of Penang Island, Malaysia. (b) Digitized Elevation Model [DEM], (c) average monthly temperature chart, and (d) average monthly precipitation chart of Penang Island, Malaysia. Inset: Location map of Peninsula Malaysia. 55

Figure 3.2 Simplified regional geological map of Peninsular Malaysia. 57

Figure 3.3 Geological map of Penang Island, Malaysia (modified after Ong, 1993). The three studied sites are indicated on the map as Site 1 (USM Main Campus), Site 2 (Binjai area of Batu Maung), and Site 3 (Jelutong). 60

Figure 3.4 Flowchart diagram of the methodological framework for the research. 62

Figure 3.5 Aerial geophysical data acquisition maps of; (a) Site 1 (USM Main Campus, including Restu Hostel), (b) Site 2 (Binjai area of Batu Maung), and (c) Site 3 (Jelutong)showing the SRT and ERT lines and borehole locations in the study area. 65

Figure 3.6 (a) ERT survey setup and the drilled borehole (BH1) at an 85 m station distance of TR1. (b) SRT survey layout showing the geophones' cable connected to grounded geophones at Site 2. (c) Image of the borehole core drilling machine and recovered samples. (d) Typical ERT layout for 2 m electrode spacing for L1, (e) 1.0 m (L4), and (f) SRT layout with 1.0 m geophone spacing for L4 at Site 3.....69

Figure 3.7 A schematic internal image of a typical ERT data acquisition system.....73

Figure 3.8 (a) A typical 2-D layout and setup for a two-cable reel measuring system. (b) Schematic diagram of a multi-electrode system and a possible 2-D measurement sequence. 74

Figure 3.9 (a) A typical SRT data acquisition layout. (b) Instrumentation and progression of seismic waves for a typical two-layered model. 75

Figure 3.10 Velocity/resistivity data inversion flowchart for the research. 78

Figure 3.11 Soil-rock conditions and quality flowchart for the study.....82

Figure 3.12 A typical RMQ chart showing the ripper performance for Caterpillar D8R/D8T and the correlation between seismic P-wave velocities and crustal materials. 83

Figure 3.13 Flowchart for the formulation and development of velocity-resistivity statistical relationships for the study. 86

Figure 4.1 Borehole lithological logs of (a–b) Site 1, (c) Lines 1–4 at Site 2, and (d–e) Site 3 in the study area. 91

Figure 4.2 Composite ERT model beneath TR1 (Site 1) at 5 m electrode spacing.....93

Figure 4.3 Composite ERT model beneath TR2 (Site 1) at 2.5 m electrode spacing.....93

Figure 4.4 Composite ERT model beneath TR3 (Site 1) at 2.5 m electrode spacing.....94

Figure 4.5 SRT model beneath TR3 (Site 1) at 2.5 m geophone spacing. 94

Figure 4.6 SRT models beneath Lines 1–4 at Site 2. 95

Figure 4.7 Composite ERT model beneath Line 3 at Site 2. 95

Figure 4.8 Composite ERT model beneath Line 4 at Site 2. 96

Figure 4.9 Composite ERT model beneath L1 at Site 3. 97

Figure 4.10 Composite ERT model beneath L2 at Site 3. 97

Figure 4.11 Composite ERT model beneath L3 at Site 3. 98

Figure 4.12 Composite ERT model beneath L3 at Site 3. 98

Figure 4.13 SRT models beneath (a) L1, (b) L2, (c) L3, and (d) L4 at Site 3.....99

Figure 4.14 ERT inversion models of TR1 with an electrode spacing of 5 m (a) and (b) TR2 with an electrode spacing of 2.5 m at Site 1. (c) Borehole lithological log of the drilled section at 85 m along TR1 in the study area. 101

Figure 4.15 (a) ERT and (b) SRT inversion models of TR3 with a station spacing of 2.5 m. (c) Nearby borehole lithological log to TR3 in the study area.....102

Figure 4.16 (a–d) SRT models of the near-surface lithologic units of Lines 1–4. (e) 3-D SRT model of Lines 1–4. (f) Borehole lithological logs of BH1–BH6 at Site 2. The dashed lines indicate fractures beneath the site. 104

Figure 4.17 Inverse model resistivity sections beneath (a) Line 3 and (b) Line 4 at Site 2. The negative station distances indicate that the ERT lines were located some stations away from the 0 m on the SRT lines. 105

Figure 4.18 (a) ERT and (b) SRT models and (c) borehole log of L1. (d) ERT and (e) SRT models of L2 in the E–W direction at Site 3 in the study area. SSSC (stiff to very stiff silty sand with little clay); VSSC (very stiff silty sand with little clay); HSSC (hard silty sand with little clay); HSSTC (hard silty sand with a trace of clay). 107

Figure 4.19 (a) ERT and (b) SRT models and (c) borehole log of L3. (d) ERT and (e) SRT models and (f) borehole log of L4 in N–S direction at

Site 3. SSSC (stiff to very stiff silty sand with little clay); VSSC (very stiff silty sand with little clay); HSSC (hard silty sand with little clay); HSSTC (hard silty sand with a trace of clay). 108

Figure 4.20 3D borehole-constrained models of ERT (a) and SRT (b) surveys at Site 3 in the study area. 109

Figure 4.21 Soil-rock models of (a) Line 1, (b) Line 2, (c) Line 3, and (d) Line 4 at Site 2. (e) 3-D soil-rock of the near-surface lithologic units beneath Site 2 in the study area. This includes the residual soil profile for comprehensive soil-rock modeling. 112

Figure 4.22 SLR plot for the RMQ of lithologic units of Site 2 in the study area. 113

Figure 4.23 RQD vs. Vp plot for RMQ of specific lithologic units in the study area. 115

Figure 4.24 The normal P-P plot of standardized regression residual for the study area. 118

Figure 4.25 Scatterplot of the regression standardized residual against regression standardized predicted value.....119

Figure 4.26 SLR plot for the RMQ of lithologic units of Site 2 in the study area. 120

Figure 4.27 RQD vs. ρ plot for RMQ of specific lithologic units in the study area. 122

Figure 4.28 Typical 2-D models generated for (a–d) the subsurface measured (borehole-based) RQD models and (e–h) estimated (SRT-based) RQD models of Lines 1–4 at Site 2 in the study area. 125

Figure 4.29 Variability model of the N-values with depths in the study area. 128

Figure 4.30 Regression plot of the N-values against their average ρ and Vp values.....130

Figure 4.31 ERT and SRT inversion models of; (a–b) Line 3 and (c–d) Line 4 at Site 2 in the study area. 132

Figure 4.32 SLR plot of the filtered velocity-resistivity datasets at Site 2.....134

Figure 4.33 (a) Histogram plot of the regression standardized residual, (b) normal P-P plot of regression standardized residual (stepwise SLR), and (c) scatterplot of the regression standardized residual against the regression of standardized predicted value for the analyzed velocity-resistivity models ($N = 110$). 138

Figure 4.34 SLR plot of the logarithm filtered velocity-resistivity data for the study area. 139

Figure 4.35 SLR plot of the velocity-resistivity data for each lithologic unit in the study area..... 141

Figure 4.36 SLR plot of the predicted and observed Vp data from unified velocity-resistivity geostatistical relationship. 144

Figure 4.37 Predicted Vp model of (a) Site 1 TR1, (b–c) predicted and observed Vp models of TR3 at Site 1, and (d–e) predicted and observed Vp models of L3 in the study area. 146

LIST OF SYMBOLS

A	Area
B	Unstandardized coefficient
β	Standardized coefficient
C, D	Internal electrode
cm	Centimeter
d	Bulk density
E	Electric field
exp	Exponential
ft	Feet
Hz	Hentz
I	Current
J	Current density
k	Geometric factor
K	Bulk modulus (modulus of incompressibility)
km	Kilometer
$km\ s^{-1}$ (km/s)	Kilometer per second
L	Length
$Log10$ (Log) or In	Logarithm function in base 10
m	Meter
mA	Milliampere
mm	Millimeter
ms	Millisecond
m/s	Meter per second
Mp	P-wave elastic modules

ρ	Electrical resistivity
ρ_a	Apparent resistivity
r	Distance between the current electrode
R	Correlation coefficient
R^2	Coefficient of determination
s (sec)	Second
t	Intercept time
V	Voltage or Potential
V_1	Velocity of the first layer
V_2	Velocity of the second layer
V_C	Potential of the internal electrode C
V_D	Potential of the internal electrode D
V_p	Seismic P-wave velocity
V_s	Seismic S-wave velocity
$V_{p_{LB}}$	95% lower confidence interval limit
$V_{p_{UB}}$	95% upper confidence interval limit
$V_{p_{RS}}$	Velocity of residual soils
$V_{p_{W/\mathrm{w}F}}$	Velocity of weathered/weathered-fractured granitic bedrock unit
$V_{p_{FB}}$	Velocity of fresh granitic bedrock
ρ_{RS}	Resistivity of residual soils
$\rho_{W/\mathrm{w}F}$	Resistivity of weathered/weathered-fractured granitic bedrock unit
ρ_{FB}	Resistivity of fresh granitic bedrock
x_c	A point current source
X_{crit}	Critical distance
z	Depth of layer

$>$	Greater than
$<$	Less than
$\leq$	Less than equal to
$\geq$	Greater than equal to
°C	Degree Celsius
∂	Del
∇	Grad (differential change)
Ω	Ohm
Ωm	Ohm meter
%	Percentage
π	Pie
Φ (or ΔV)	Potential difference
λ	Lamé's constant
μ	Shear modulus (rigidity modulus)
φ	Poisson's ratio
$\sum$	Summation

LIST OF ABBREVIATIONS

2-D	Two-Dimensional
3-D	Three-Dimensional
4-D	Four-Dimensional
ANOVA	Analysis of Variance
BH or BHs	Borehole or Boreholes
C (1, 2) and P (1, 2)	Current and Potential Electrodes
DC	Direct Current
D-W	Durbin-Watson
EM	Electromagnetic
ERM	Electrical Resistivity Method
ERT	Electrical Resistivity Tomography
E-W	East-West
EWS	Wenner-Schlumberger Electrode Protocol
F-T	Freezing-Thawing Cycles
IFF	If and only if
IP	Induced Polarization
HSSC	Hard silty sand with little clay
HSSTC	Hard silty sand with a trace of clay
MASW	Multichannel Analysis of Surface Waves
MLR	Multiple Linear Regression
N-S	North-South
N-value	A measure of penetration resistance
P-waves	Compressional, longitudinal, or primary waves
RIOT	Refraction Inversion and Optimization Technique

RMQ	Rock Mass Quality
RMSE	Root Mean Square Error
RQD	Rock Quality Designation
RST	Restu Hostel, USM
SLR	Simple Linear Regression
SP	Spontaneous Potential (Self potential)
SPSS	Statistical Package for Social Sciences
SPT	Soil Penetration Test
SRT	Seismic Refraction Tomography
SSSC	Stiff to very stiff silty sand with little clay
S-waves	Shear, transverse, or secondary waves
TT	Transit times
USM	Universiti Sains Malaysia
VIF	Variance Inflation Factor
VSSC	Very stiff silty sand with little clay
W-D	Wetting-Drying Cycles
W-D-F-T	Wetting-Drying- Freezing-Thawing Cycles

LIST OF APPENDICES

Appendix Table A1	Typical soil descriptive analyses at different depths for boreholes in the study area.
Appendix A1	A Typical ERT model of TR1 at site 1 for 5 m electrode spacing before filtering.
Appendix A2	A Typical ERT model of TR2 at site 1 for 2.5 m electrode spacing before filtering.
Appendix B1	The model block and apparent resistivity datum point (top panel), inversion model resistivity section (middle panel), and model block relative sensitivity section (bottom panel) of TR1 at site 1.
Appendix B2	the model block and apparent resistivity datum point (top panel), inversion model resistivity section (middle panel), and model block relative sensitivity section (bottom panel) of TR2 at site 1.
Appendix C	A typical seismic velocity raypath model of Line 3 (Site 2)
Appendix D	Final inverted SRT model beneath Line 1 At Binjai, Batu Maung (Site 2).
Appendix Table A2	Estimated RQD and their velocity values at BH1–BH4 along Lines 1 and 2 in the study area.
Appendix Table A3	Estimated RQD and their resistivity and velocity values at BH1, BH3, and BH5 along Line 3 in the study area.
Appendix Table A4	Estimated RQD and their resistivity and velocity values at BH2, BH4, and BH6 along Line 3 in the study area.
Appendix Table A5	Estimated RQD and their corresponding velocity and resistivity values.
Appendix E	Typical borehole log sheet for BH1 at Site 3 in Jelutong
Appendix Table A6	SPT (N-values) results of borehole-derived samples based on blows per 30 cm, with their resistivity and velocity values in the study area.
Appendix Table A7	Summary of the estimated N-values against their average resistivity and velocity values.

Appendix F1	Generated mesh models of the (a) resistivity and (b) seismic velocity datasets. (c) Collocated velocity-resistivity mesh of Line 3.
Appendix F2	Generated mesh models of the (a) resistivity and (b) seismic velocity datasets. (c) Collocated velocity-resistivity mesh of Line 4.
Appendix Table A8	Summary of the filtered resistivity-velocity data and their predicted velocities at Site 2.
Appendix Table A9	Selected velocity-resistivity data for determining the empirical relationships for the specific lithologic units.

PEMBANGUNAN PERHUBUNGAN NOVEL GEOFIZIK–GEOTEKNIKAL PERSEKITARAN GRANITIK DI PULAU PINANG, MALAYSIA

ABSTRAK

Pencirian keadaan batuan tanah berhampiran permukaan adalah mencabar dalam rupa bumi kristal tropika disebabkan oleh geologi yang kompleks dan kekurangan penanda stratigrafi yang berbeza. Ciri-ciri ini boleh dipetakan secukupnya menggunakan perhubungan halaju-kerintangan melalui pemodelan kualiti batu-tanah yang dioptimumkan secara statistik, terutamanya di kawasan yang mempunyai beban atas <50 m. Pendekatan ini belum pernah digunakan di kawasan granitik tropika. Bagi mencapai matlamat penyelidikan, Pulau Pinang, Malaysia terain granitik tropika, dianggap sebagai kawasan yang sesuai kerana ciri-ciri batuan tanah intrinsiknya dan keperluan untuk menyelesaikan isu berkaitan alam sekitar. Oleh itu, penyelidikan ini membangunkan hubungan statistik halaju-kerintangan untuk rupa bumi granit berdasarkan pemodelan geotomografi yang kompleks (tomografi kerintangan elektrik dan tomografi biasan seismik [SRT]). Untuk tujuan ini, empat senario metodologi terperinci telah digunakan, memanfaatkan log lubang gerudi, penetapan kualiti batuan (RQD), ujian penembusan tanah (nilai N-SPT), dan analisis regresi yang diselia. Keputusan menunjukkan bahawa log litologi lubang gerudi berkorelasi baik dengan model litologi berasaskan kerintangan dan SRT di bahagian timur (Sungai Ara), selatan (Batu Maung), dan utara (Jelutong) Pulau Pinang. Kawasan ini dicirikan oleh tanah atas kelodak berpasir, pasir berkelodak kepada unit terluluhawa berpasir, unit terluluhawa/pecah dan batuan dasar granitik integral/segar. Penilaian kualiti batuan, melalui RQD berasaskan lubang gerudi, dan model RQD berasaskan SRT dan kerintangan, mempunyai ketepatan ramalan empirikal 95.8% hingga 100%. Nilai-N

SPT berasaskan lubang gerudi juga mewujudkan korelasi yang signifikan dengan model SRT yang diperhatikan. Akhirnya, hubungan statistik halaju-kerintangan berasaskan litologi bersatu mempunyai ketepatan ramalan > 85% walaupun litologi kawasan kajian itu rumit. Tiga perhubungan statistik halaju-rintangan berasaskan litologi khusus meningkatkan ketepatan ramalan kepada> 98%. Oleh itu, rangka kerja metodologi berbantukan statistik yang komprehensif dan perhubungan empirikal kerintangan halaju yang diperolehi boleh digunakan dalam terain granit tropika yang setanding untuk pemodelan batuan tanah berhampiran permukaan. Kebolehgunaan model berasaskan litologi yang diukur dan diramalkan telah disesuaikan untuk menyelesaikan reka bentuk infrastruktur. Berdasarkan keputusan keseluruhan, infrastruktur kejuruteraan harus menggunakan cerucuk yang dibenamkan, sebaiknya, ke batuan dasar granit yang segar dengan kedalaman antara 12–40 m. Ini disebabkan oleh kekuatan galas beban yang rendah bagi unit litologi yang dikaitkan dengan tanah liat/kelodak dan badan yang berpotensi mengandungi air. Paling penting, kajian ini telah merapatkan jurang antara ahli geofizik dan geo-jurutera dengan mewujudkan pemodelan ramalan halaju-rintangan yang baru dan kos rendah yang dioptimumkan secara statistik, terutamanya untuk kawasan yang luas tanpa data lubang gerudi atau terhad.

DEVELOPMENT OF NOVEL GEOPHYSICAL–GEOTECHNICAL RELATIONSHIPS OF GRANITIC ENVIRONMENTS IN PENANG ISLAND, MALAYSIA

ABSTRACT

The characterization of near-surface soil-rock conditions is challenging in tropical crystalline terrains due to complex geology and lack of distinct stratigraphic markers. These features can adequately be mapped using velocity-resistivity relationships via statistically optimized soil-rock quality modeling, especially in areas with overburden <50 m. The approach has not been used in tropical granitic terrains. To achieve the research goals, Penang Island, Malaysia; a tropical granitic terrain, was considered a suitable area due to its intrinsic soil-rock characteristics and the need to resolve environmental-related issues. This research, therefore, develops velocity-resistivity statistical relationships for granitic terrains based on complex collocated geotomographic (electrical resistivity tomography and seismic refraction tomography [SRT]) modeling. To this end, four detailed methodological scenarios were utilized, leveraging borehole logs, rock quality designation (RQD), soil penetration test (SPT N-values), and supervised regression analysis. The results show that the borehole lithologic logs correlate well with resistivity- and SRT-based lithological models at the eastern (Sungai Ara), southern (Batu Maung), and northern (Jelutong) sections of Penang Island. The areas are characterized by sandy silt topsoil, silty sand to sandy weathered units, weathered/fractured units, and integral/fresh granitic bedrock. The rock quality assessment, via borehole-based RQD, and SRT- and resistivity-based RQD models, had empirical prediction accuracies of 95.8% to 100%. The borehole-based SPT N-values also established significant correlations with the observed SRT

models. Ultimately, the unified lithology-based velocity-resistivity statistical relations had prediction accuracies of >85% despite the complexity of the study area's lithologies. The three specific lithology-based velocity-resistivity statistical relations enhanced the prediction accuracy to >98%. Thus, the comprehensive statistically-assisted methodological framework and the derived velocity-resistivity empirical relationships can be used in comparable tropical granitic terrains for near-surface soil-rock modeling. The applicability of the measured and predicted lithology-based models was adapted to resolving infrastructure design. Based on the overall results, engineered infrastructure should be piled, preferably, to the fresh granitic bedrock with depths ranging from 12–40 m. This is due to the low load-bearing strength of the lithologic units attributable to clay/silt and potentially water-containing bodies. Most importantly, this study has bridged the gaps between geophysicists and geo-engineers by establishing novel, low cost statistically optimized velocity-resistivity predictive modeling, particularly for large aerial extents with no or limited borehole data.

CHAPTER 1

INTRODUCTION

1.1 Background

In geoscience, multi-geophysical imaging, powerful data inversions, and analytical methods are increasingly important. This field of science uses cutting-edge surveying, inversion, supervised and unsupervised machine learning, and statistical techniques (especially regression) for data- and image-driven analyses (Meju et al., 2003; Gallardo & Meju, 2007; Bery & Saad, 2012a, 2012b; Merritt, 2014; Merritt et al., 2014; Meju & Gallardo, 2016; Hasan et al., 2017, 2018, 2020a, 2020b, 2021a). All these powerful problem-solving approaches can be employed for all geophysical methods. Indirect and direct geophysical methods, particularly seismic and electrical methods, are often used to measure the physical and geomechanical properties of surficial and subsurface geology at different spatial and temporal scales (Budetta et al., 2001; Cardarelli & Di Filippo, 2009; Kalantary et al., 2009; Olayanju et al., 2017; Rønning et al., 2019; Adiat et al., 2020; Suzuki et al., 2021; Hasan et al., 2022a).

The possibility of achieving accurate predictions of geologic characteristics requires detailed multidimensional geophysical inversion modeling. However, the use of diverse geophysical datasets from related and unrelated physical events is a major challenge (Sivrikaya & Toğrol, 2006; Bery, 2016a, 2016b; Rymarczyk et al., 2019, 2021; Hasan & Shang, 2022). This matters because of the contrasts in measured parameters, model complexities, and model uncertainties, among others (Reynolds, 1997; Gallardo & Meju, 2007, 2011). To this end, selecting appropriate geophysical methods with the right imaging spacings is pertinent for improved subsurface geological investigations, particularly in exploration/environmental studies, infrastructure design, subsurface simulations, etc. These are highly essential in

improving data resolution, signal-to-noise ratio, project turnaround time and cost implications, and overall production results (Barton, 2006; Griffith & King, 2011; Kumar et al., 2016; Hasan et al., 2022a; Hasan & Shang, 2022). Seismic refraction and electrical resistivity techniques have so far contributed significantly to the above advantages, particularly in near-surface and relatively deep crustal studies. Traditionally, the seismic P-wave velocity (V_p) and electrical resistivity (ρ) models can be diagnostic independently. However, their improved techniques, i.e., seismic refraction tomography (SRT) and electrical resistivity tomography (ERT), provide detailed and reliable surficial to subsurface soil-rock features, both laterally and vertically nowadays (Quigley, 2006; Loke et al., 2013; Dahlin & Wisén, 2018; Ronczka et al., 2018; Akingboye et al., 2022).

In recent years, SRT has become more popular for two-dimensional (2-D) subsurface crustal investigations. It effectively delineates weathered layers, water tables, bedrock structures, and soil-rock interfaces as well as for correcting structure-related problems in reflection models. It is also used indirectly to determine rock mass rippability or rock mass quality (RMQ) (El-Naqa, 1996; Hoek & Brown, 1997; Hashemi et al., 2010; Ismail et al., 2018a; Zhang et al., 2019; Jug et al., 2020; Gottron & Henk, 2021). The three- and four-dimensional (3-D and 4-D) SRT surveys are still in the initial research stages (Lin et al., 2015). Defining specific lithologies is challenging via SRT due to masked zone, overburden of less than 50 m, hidden layers (i.e., a layer of low velocity beneath a high-velocity layer), and sections with water infills (Quigley, 2006; Bery, 2013; Hiltunen et al., 2007; Akingboye & Ogunyele, 2019). These issues can result in the inaccurate delineation of the near-surface soil-rock profiles and formation architecture. The problems can be annulled by using additional complementary methods. ERT, one of the best complementary techniques,

can adequately compensate for the limitations of the seismic refraction method. The integration of both methods provides adequate aids in mapping discrete soil profiles, rock boulders (floaters), caverns, karst voids, pollution plumes, and air- and water-filled voids, among others (Barton, 2006; Ronczka et al., 2017, 2018; Cheng et al., 2019; Zhao et al., 2019; Christensen et al., 2020).

ERT is a versatile noninvasive technique with a wide range of resistivity values due to the coexisting relationships between varying subsurface lithologies and resistivities. The technique can be used effectively at the earth's surface, in boreholes (or cross-holes), and at the surface and bottom of streams/rivers (Dahlin, 1996; Bery & Saad, 2012b; Ganerød et al., 2006; Loke et al., 2013; Akingboye et al., 2022). Due to the technique's field data acquisition speed with low-cost surveying design, especially in 3-D ERT surveys, it has been widely adopted in small and large-scale investigations (Nordiana et al., 2013; Dahlin & Loke, 2018; Cheng et al., 2019; Hung et al., 2019, 2020; Akingboye et al., 2022). A 4-D ERT survey (or time-lapse ERT) now provides more desired information on complex terrains and spatiotemporal water/moisture changes by measuring resistivity variations over days, weeks, months, or years (Barker & Moore, 1998; Merritt, 2014; Bery, 2016b; Alamry et al., 2017; De Carlo et al., 2020; Bièvre et al., 2021; Loke et al., 2022). Nevertheless, the ambiguities in geological interpretations put the ERT technique to the test. For instance, increasing ion concentration in water-saturated or clay-rich sandy formations can produce a low resistivity anomalous feature. In addition, lithological characteristics, pore fluid chemistry, void spaces, and other factors impact resistivity response. Thus, measured chargeability from the induced polarization (IP) survey (Slater et al., 2000; Slater & Lesmes, 2002; Slater & Glaser, 2003; Binley & Kemna, 2005; Rey et al., 2020) and borehole-derived soil-rock logs, rock quality designation (RQD), and *in situ* soil

penetration tests (SPT N-values) can settle these uncertainties (Braga et al., 1999; Sivrikaya & Toğrol, 2006; Kumar et al., 2016; Hasan & Shang, 2022). The relationships between velocity and resistivity (here-in-after referred to as velocity-resistivity) data with any of the above uncertainty-resolving techniques can provide more robust and detailed soil-rock information than their independent models.

Interestingly, discussions on velocity-resistivity relationships in geosciences and other related fields are currently underway to provide a fundamental law connecting velocity and resistivity parameters. Thus far, the interpretations of velocity-resistivity relationships have been based on interpolated (or co-analyzed) 2-D modeling with statistical/numerical analysis, e.g., (Meju et al., 2003; Colombo et al., 2008a; Meju & Gallardo, 2016; Ronczka et al., 2017; Zeng et al., 2018). However, the 3-D statistical modeling approach is still evolving. The collocation of seismic velocity and resistivity models is becoming commonplace for developing robust analytical inversion and interpretation schemes in subsurface characterization (Meju et al., 2003; Gallardo, 2004; Gallardo & Meju, 2003, 2007; Gunther et al., 2006; Zeng et al., 2018). Soil-rock porosity is a typical assumption aiding velocity-resistivity relationships as an effective geophysical analytical tool. This property considerably influences compressional velocities and conductivities due to soil-rock matrix fraction against fluid (Meju et al., 2003; Gunther et al., 2006; Gallardo, 2007; Gallardo & Meju, 2003, 2007, 2011; Yoon & Lee, 2010; Bery & Saad, 2012b; Lee & Yoon, 2015; Meju & Gallardo, 2016; Ronczka et al., 2017, 2018).

Most importantly, the information derived from RQD and SPT N-values via borehole geotechnical tests is critical in understanding soil-rock conditions and their architectures. These parameters are key in the collocation or simultaneous joint

inversion of seismic velocity and resistivity datasets. RQD and N-value models offer the spatial determination of soil-rock integrity, soil strength, rock fractures, water- or soil-filled zones, etc (Ramamurthy, 2004; Barton, 2006; Butchibabu et al., 2017; Pells et al., 2017; Hasan et al., 2021b, 2022a;). The soil-rock integrity procedures will significantly improve the measured and predicted models from velocity-resistivity relationships to accurately delineate lithology, pore fluids, rock fracturing spatial variation, hidden thin velocity layers, and environmental-related issues in this research. However, previous researchers have not experimented with the soil-rock quality approach in developing velocity-resistivity statistical relations. This is because it is challenging to determine physical, geomechanical, and hydrogeological characteristics from conventional borehole drilling tests due to cost implications for large aerial extent (Bery & Saad, 2012a; Akingboye & Ogunyele, 2019; Hasan et al., 2020b, 2022a).

Consequently, the study area (Penang Island, Malaysia) is an ideal geological setting for evaluating this hypothesis and developing novel velocity-resistivity statistical relationships for tropical granitic terrains. Despite the enormous benefits of velocity-resistivity relationships in some terrains, e.g., (Colombo et al., 2008b; Meju et al., 2003; Meju & Gallardo, 2016; Zeng et al., 2018), researchers are yet to adopt this problem-solving technique in tropical granitic terrains, especially Penang Island, Malaysia. In addition, no definitive velocity-resistivity statistical relationships have been developed. However, SRT and ERT have been used to evaluate the properties of granitic rocks, e.g., (Zhao et al., 1994; Olona et al., 2010; Bery & Saad, 2012b; Balarabe & Bery, 2021; Balarabe et al., 2022). This research is, therefore, the next step in improving soil-rock characterization using a novel approach that integrates lithology-based borehole tests, complex collocated velocity-resistivity technique, and

supervised regression modeling. The first criteria used to achieve the velocity-resistivity relationships were borehole-derived logs, RQD, and SPT N-value data of the complex near-surface lithologic units. These, including predicted velocity models, were also used to assess the study area's spatial surficial and subsurface soil-rock conditions on a large scale. This novel study is the first of its kind in Penang and, most notably, in tropical granitic terrains.

In contrast to earlier researchers, the complex collocated velocity-resistivity modeling approach for this study used dual spacings with a slight difference in station intervals. This is envisaged to make the empirical relationships developed work effectively for models of different station spacing scenarios. A complete methodological framework that includes simultaneous velocity-resistivity inversion and supervised regression workflows to achieve robust and accurate statistical relationships for effective use in granitic terrains, was also developed. This research also leveraged various statistical techniques to verify the accuracy of the derived empirical relations as well as measured and predicted models. The research findings adequately define the physical, hydrogeological, and geomechanical of the study area's soil-rock conditions to mitigate environmental issues, particularly infrastructure design. This research will bridge the gap between geophysicists and geo-engineers (and hydrogeologists) by offering novel, low cost statistical-assisted geophysical-geoengineering techniques for optimizing soil-rock characterization in tropical granitic terrains, particularly areas with an overburden of less than 50 m and places borehole data are limited or unavailable.

1.2 Problem Statement

The characterization of surficial and subsurface soil-rock conditions in tropical crystalline basement terrains is challenging due to varying weathering conditions, localized structures, and the absence of distinctive stratigraphic markers (Bery & Saad, 2012a, 2012b; Lee et al., 2021; Hasan et al., 2022a, 2022b, 2022c). As a result, geoscientists and related disciplines have used cutting-edge geophysical and inversion (with optimized analytical) techniques to resolve such problems. This is because noninvasive geophysics provides volumetric subsurface measurements with no disruption (Chambers et al., 2006; Naudet et al., 2008; Maślakowski et al., 2014; Loperte et al., 2016; Osinowo & Falufosi, 2018; Cheng et al., 2019; Christensen, 2022). However, detailed and predictive geophysical modeling approaches are required for dense, detailed soil-rock characterization, e.g., (Gallardo & Meju, 2003; Colombo et al., 2010), particularly in the study area.

Resolving soil-rock-related environmental issues requires a broad knowledge of the surface-to-subsurface geologic conditions via an integrated novel approach rather than relying on previous piecemeal research in the study area and its environs, e.g., (Bery & Saad, 2012a; Ismail et al., 2018a, 2018b; Aziman et al., 2019; Balarabe & Bery, 2021; Salleh et al., 2021; Zakaria et al., 2021, 2022; Balarabe et al., 2022). Despite the benefits of ERT and SRT with statistical relationships, e.g., (Marquis & Hyndman, 1991, 1992; Gallardo & Meju, 2007; Zeng et al., 2018), co-analyzing both parameters via empirical relations has not been practicalized in tropical granitic terrains, particularly the study area. As this is a complex modeling procedure that requires high expertise to prevent net loss of data and also to derive a high prediction accuracy for modeled soil-rock conditions, most especially in areas with overburden <50 m. Hence, a need for complex collocated velocity-resistivity modeling using

proven geophysical station intervals (or spacings) and effective statistical analyses to fully address varied soil-rock conditions. This predictive modeling approach is achievable typically based on the assumption that velocity-resistivity relationships are a porosity factor in noninvasive subsurface investigations (Eberhart-Phillips et al., 1995; Meju et al., 2003; Gallardo & Meju, 2003, 2007; Zeng et al., 2018).

Furthermore, the independent correlation of V_p with RQD (Barton, 2006; Griffith & King, 2011; Bery & Saad, 2012a; Abzalov, 2016) and N-values (Hasancebi & Ulusay, 2007; Akin et al., 2011; Kumar et al., 2016; Alkhamaiseh et al., 2018), and the correlation of ρ with RQD (Hasan et al., 2021b; 2022a, 2022b) can provide standardized parametric geotechnical results for areas with few or no borehole data and in highly steep regions where borehole drilling is impossible (Ramamurthy, 2004; Sivrikaya & Toğrol, 2006; Bery & Saad, 2012a; Kumar et al., 2016; Lin et al., 2017; Salaamah et al., 2019). These soil-rock parametric factors derivable from empirical relations, especially ρ with RQD, are yet to be deduced for tropical granitic terrains.

Given the above, Penang Island, the preferred study area to demonstrate and develop the objectives of this research, is a small area in Malaysia with a typical wet tropical climate having high annual rainfall and sun intensity. The seasonal variations of these tropical climates and other geologic activities have aided the progressive weathering of rock minerals, resulting in varying complex soil-rock profiles with locations (Bery et al., 2011; Bery, 2016a). As a result, the study area's small landmass is much sought after for urbanization. Increased industrialization activities and the growth of other economic sectors have currently led people to build high-rise structures, with many projects to be executed in the future on the island. Lack of proper soil-rock characterization in the study area could cause structural failure arising from

ignorance of geological uncertainties in foundation rocks (Habibu & Lim, 2016; Ismail et al., 2018a; Lee et al., 2021; Salleh et al., 2021; Zakaria et al., 2021). Therefore, co-analyzing velocity-resistivity optimized models and engineering data (RQD and SPT N-values) is a giant leap forward in resolving this problem and other soil-rock-related environmental issues. This will accurately improve the 2-D/3-D modeling and delineation of physical, geomechanical, and hydrogeological features over a large aerial extent in the study area and places with similar geology.

1.3 Research Justification

The non-existence of a fundamental law for velocity-resistivity data/models have stirred the interests of many researchers to provide correlations from their simultaneous/joint inversion, modeling, or statistical data clustering/relationships, e.g., (Opfer, 2003; Colombo & De Stefano, 2007; Colombo et al., 2008a, 2008b, 2010; Muñoz et al., 2010). Also, due to the lack of effective theoretical correlation formulations between *in situ* geotechnical tests and soil engineering parameters coupled with the costs of borehole drilling, the only credible approach to determining spatial soil-rock integrity is by developing empirical relations. This is effective for co-analyzing RQD and N-values with V_p and ρ via statistical (regression) analyses, e.g., (Sivrikaya & Toğrol, 2006; Kalantary et al., 2009; Bery & Saad, 2012a; Kumar et al., 2016). These techniques can offer robust 2-D/3-D models of the near-surface, providing a detailed understanding of soil-rock variability and their interfaces to mitigate infrastructure failure, landslides, soil liquefaction, groundwater deficit, etc (Kalantary et al., 2009; Bery & Saad, 2012a; Priya & Dodagoudar, 2015; Syukri, 2020; Hasan et al., 2022a). Similarly, velocity-resistivity relationships have been applied to geologic conditions, such as dry, wet, frozen, and thawed conditions, as well as in

some sedimentary and crystalline basement terrains. The resulting empirical trends related to porosity, water saturation, sand-filled fractures, and subsurface geologic boundaries have also been evaluated (Marquis & Hyndman, 1992; Gallardo & Meju, 2003, 2004, 2007; Gunther et al., 2006; Yao et al., 2017).

Logically, supposedly that geotechnical approaches and velocity-resistivity statistical modeling and prediction could address environmental problems in terrains where they were employed. In that case, these techniques with optimized statistical analyses and empirical predictive modeling should also be effective in granitic terrains. Therefore, the need to develop this problem-solving statistically optimized geophysical techniques in a typical granitic terrain in the tropics. The developed statistically-assisted velocity-resistivity relationships will help reduce the uncertainties for the successful construction of infrastructure and mitigation of ground-induced failure in the study area and other terrains with the same geologic characteristics. Overall, it will drastically reduce the high costs of drilling boreholes, ambiguities in geological model interpretation, and laborious field exercises for reliable determination of soil-rock conditions, thereby giving relief to geoscientists. Also, since the techniques are fast, cost-effective, and have a wide range of values to characterize subsurface geologic features, the research novel approach will adequately resolve soil-rock-related environmental issues.(Kuras et al., 2016; Dahlin & Loke, 2018; Ronczka et al., 2018; Akingboye & Ogunyele, 2019; Aziz et al., 2019; Holmes et al., 2020;Balarabe et al., 2022).

1.4 Research Objectives

The specific objectives of the research are:

i. to develop effective lithology-based statistical relationships for V_p and ρ with RQD and SPT N-values for granitic terrains;

ii. to develop robust statistically-assisted geophysical workflows and empirical relations for co-analyzing V_p and ρ via complex collocated modeling with optimized linear regression analyses, and

iii. to evaluate and define the range of V_p and ρ for the surficial to subsurface soil-rock units based on SRT and ERT models and objectives (i) – (ii).

1.5 Research Questions

The following research questions are intended to be answered as they serve as motivation for this research:

i. Which geotomographic approach between ERT and SRT provides the best soil-rock characterization models in tropical granitic terrains?

ii. Can the performance of tomographic methods be improved to increase the resolution and quality of measured velocity and resistivity data for the same coincident model grids or pixels?

iii. Are there any statistical correlations between V_p and ρ of subsurface lithological distributions in granitic terrains?

iv. Are the delineated velocity-resistivity trends in this study consistent with those obtained in different geological terrains/conditions? If not, what could have caused the variation?

v. Do the lithology-based empirically derived models outperform their measured models, and are they efficient in accurately predicting and offering problem-solving subsurface information?

1.6 Scope of the Study

The scope of this research focuses on the development of velocity-resistivity geostatistical relationships for effective surficial and subsurface soil-rock characterization in complex tropical granitic terrains. To successfully achieve this, combined detailed soil-rock quality (RQD and SPT N-value) modeling, complex collocated V_p and ρ modeling, and the optimization power of supervised regression analysis, were used. To achieve the research goals, Penang Island in Malaysia; a tropical granitic terrain, was considered a suitable area due to its intrinsic soil-rock characteristics and the need to resolve environmental-related issues. Three sites: two (Sites 1 and 3) in the North Penang Pluton and one (Site 2) in the South Penang Pluton, will be investigated to design and achieve the research objectives.

For potential results optimization, this study is segmented into stages: 1) reconnaissance surveys and performance assessment of used geotomographic electrodes; 2) detailed field geophysical (ERT and SRT) and geotechnical (RQD and SPT N-value) surveys; 3) detailed geophysical data inversions, soil-rock quality modeling, and complex collocation and development of velocity-resistivity geostatistical relationships; and 4) statistical optimization of soil-rock quality and velocity-resistivity relationships as well as assessing their performances in soil-rock

modeling and prediction. This will overall help assess the impacts of the delineated lithologies and geohydrodynamic-controlled structures from the derived and predicted models on infrastructure design.

While this research aims to provide the above-mentioned valuable insights in tropical granitic terrains, it does not cover other environmental problems such as groundwater modeling and landslide occurrence determination as well as other crystalline basement or sedimentary terrins and deep crustal investigations in excess of several hundreds of meters and kilometers. Additionally, the study will not delve into evaluating the accuracy and performances of the developed statistically optimized soil-rock and velocity-resistivity relationships outside the terrain of Penang Island. This is due to the choice of rock type and, most especially, the cost implication.

The research findings can contribute to the existing literature on characterizing complex near-surface soil-rock conditions and qualities, as well as developing statistically optimized velocity-resistivity relationships in tropical granitic terrains. However, the generalization of results beyond the specified statistical-assisted soil-rock methodological framework and the geographical area should be approached with caution.

1.7 Motivation of the Study

The desire for more efficient and adaptive statistically optimized data- and image-based geophysical models are evolving to solve environmental issues. However, these methods are site-specific and function admirably in different terrains. The importance of electrical resistivity and seismic refraction methods in subsurface crustal studies is enormous. In terms of near-surface field data acquisition and data inversion processes, both SRT and ERT are easy to perform and modify to solve many

environmental problems. In addition, the methods are cost-effective and rapid to achieve the expected project plan's turnaround time as well as produce quality results with a higher success rate for soil-rock definition.

As previously stated, borehole geotechnical tests for soil-rock quality require heavy equipment with high costs and cannot be deployed on steep terrains. Hence, spatial variability of soil-rock conditions and quality can be predicted from effective empirical relations of V_p and ρ with RQD or N-values. Similarly, the velocity-resistivity relationships have been employed to tackle geophysical problems under different geologic conditions. If such an approach were effectively utilized in some areas, its statistically optimized relationships could be adaptive in granitic terrains. Determining soil-rock parameters in granitic terrains with high accuracy via the approach will be a significant accomplishment in environmental studies.

The chosen study area (Penang Island, Malaysia) has all of the required surficial and subsurface soil-rock characteristics for a typical tropical climate region. The proximity of study sites regarding research timeframe, availability of borehole data, cost of deploying field equipment and personnel, nature of the geological terrain, and success stories from previous studies on various environmental problems all played a significant role in the study location selection.

1.8 Thesis Layout

Chapter 1 presents the research background, focusing on the broad relevance of velocity-resistivity relationships in subsurface characterization. The section also highlighted the advantages and disadvantages of ERT and SRT, the fundamental constraints in developing velocity-resistivity relations, and their independent correlations with RQD and N-values. The statement of the problem, justification,

specific objectives, scope, and motivation of the research, including research questions, for developing velocity-resistivity statistical relationships in granitic environments were also explicitly highlighted.

In Chapter 2, detailed literature reviews on ERT, SRT, soil-rock qualities (RQD and SPT N-values), and velocity-resistivity statistical formulations and relationships to support the background of the study were presented. Benefits and gaps in previously reviewed studies were emphasized. Therefore, to achieve the study's objectives and highlight the novelty and contributions of the research, this study is designed on the identified gaps.

Chapter 3 presents extensive and detailed discussions on the location, geography, relief, and regional and local geology of the study area. Concise, yet adequate, elucidation on the employed methods (V_p, ρ, RQD, and SPT N-values), and the development of a complete methodological, velocity-resistivity inversion, and supervised regression workflows are also presented. The formulation and collocation of V_p and ρ mesh models, the development of empirical relations for V_p and ρ with RQD and SPT N-values, as well as velocity-resistivity statistical relationships for granitic terrains, are also presented in this chapter.

The research results and their detailed discussions are presented in Chapter 4. The chapter also explicitly presents the novelties of the research and their overall contribution to existing knowledge. The limitation of the research is also highlighted.

Chapter 5 presents the study's conclusions and recommendations for future research.

CHAPTER 2

LITERATURE REVIEW

2.1 Introduction

This section reviews previous works on electrical resistivity and seismic refraction techniques in near-surface crustal studies. Reviews on the theories and principles influencing electrical resistivity (or conductivity) and seismic refraction as well as their general applications are presented. In addition, the statistical relationships between these two geophysical parameters, which can also be referred to as velocity-resistivity statistical relationships, in different terrains, and under different geologic conditions, are also reviewed. The reviews aim to identify gaps in previous studies. This way, the relevance and the novelties of the proposed research study will be helpful as inputs for designing problem-solving methodologies (preliminary and detailed field data gathering techniques, data processing, efficient statistical analyses, and modeling) and interpreting the research results.

2.2 An Overview of Electrical Resistivity Methods

Since the early 1920s until the late 1980s, the electrical resistivity method (ERM) has been the primary and most widely utilized 1D imaging technique (Griffiths et al., 1990; Aizebeokhai, 2010). The 1-D is a single probing method and as such is insufficient in resolving complex subsurface geology considerably. Over the years, the field of electrical resistivity imaging has significantly improved to provide 2-, 3-, and 4-D subsurface crustal models.

Natural fields within the earth and artificially generated currents injected into the earth's formation are used in electrical surveying methods. ERM provides the

apparent resistivity, ρ_a, (or conductivity σ) of surficial and underlying crustal materials and water-saturating fills via artificially generated current (Loke et al., 2013; Ronczka et al., 2017). Two current electrodes are used to inject electrical current into the subsurface, and another two electrodes measure the resulting potential difference (voltage). This allows for the calculation of ρ_a, taking into account the resistance for a precise measurement of a homogenous layer. Since increasing separation leads to greater depth penetration, the field-measured apparent resistivity is used to produce a composite resistivity image (consisting of the measured and calculated apparent resistivity pseudosections and inverse model resistivity section) of near-surface soil-rock conditions for the area investigated. As a result, the generated inverse model resistivity section displays the variations in resistivity responses associated with subsurface lateral and vertical soil-rock profiles with their interfaces (or boundary conditions) and structures, as well as delineating water- and air-filled sections, boulders, and cavities (Crook et al., 2008; Akingboye & Ogunyele, 2019; Binley & Slater, 2020). Apart from the highlighted applicability of ERM, the method has numerous benefits in near-surface crustal investigations.

2.2.1 Theories and Principles of Electrical Resistivity Methods

Ohm's law governs the link between electrical resistivity, current, and potential. The potential difference is determined for a point current source at x_c in a continuous medium based on two theories: Ohm's law and Poisson's equation for current conservation (Telford et al., 1990; Loke et al., 2013). The combined expression given in Equation 2.1 can be simplified as the fundamental principle on which the resistivity data acquisition and interpretation depend.

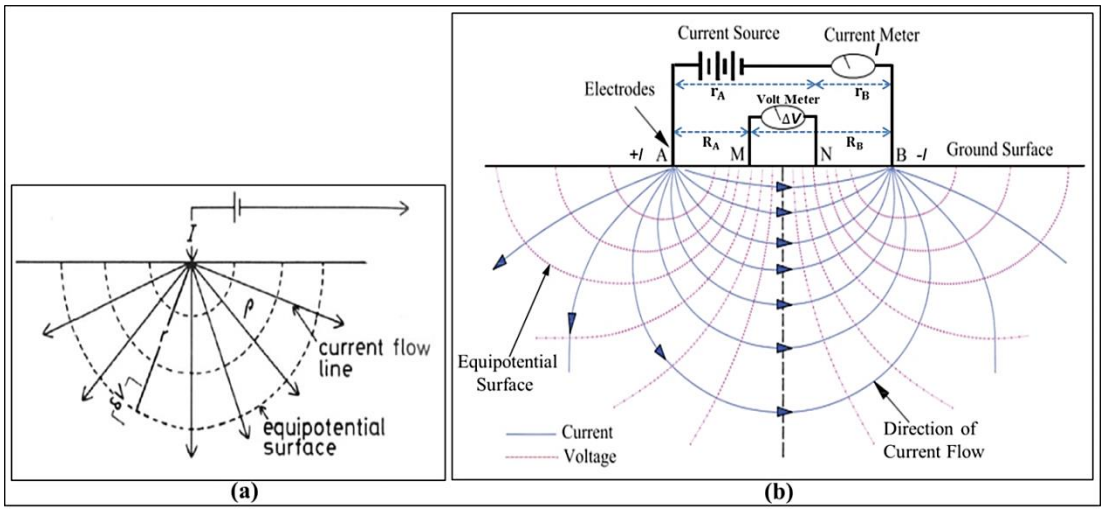

Figure 2.1 (a) A single-point source electrode with electric flow current in the subsurface. (b) A schematic fundamental diagram of a four-electrode resistivity measurement at the earth's surface and the subsurface distribution of the generated current flow.

$$\nabla.\left[\frac{1}{\rho(x,y,z)}\nabla\Phi\psi(x,y,z)\right] = -\frac{\partial J}{\partial t}\partial x_c \tag{2.1}$$

Where ρ is the resistivity, Φ is the potential, and J is the current density.

Taking the earth as a hemispherical shell with a uniform ρ from a single grounded current electrode (Figure 2.1a), the current flows radially into the subsurface. This allows a uniform current distribution. The hemispherical shell then has a surface area of $A = 2\pi r^2$ at a distance r from the electrode to give the current density (J), as given in Equation 2.2.

$$J = \frac{I}{A} = \frac{I}{2\pi r^2} \tag{2.2}$$

The charge density can also be given as $J = \frac{E}{\rho}$;

Where $E = -\nabla V$ (2.3)

E is referred to as the electric field or the gradient of a scalar potential.

Hence, the potential gradient associated with the current density (J) is given as:

$$\nabla\Phi = -\rho J = -\frac{\rho I}{2\pi r^2} \tag{2.4}$$

The potential is obtained through the integration of the following:

$$V = \int \nabla\Phi = -\int \frac{\rho I \partial r}{2\pi r^2} = \frac{\rho I}{2\pi r} \tag{2.5}$$

The general equation for a four-electrode resistivity measurement in terms of apparent resistivity and potential difference (ΔV), as shown in Figure 2.1b, is given by Equation 2.6. The potential V_M at an internal electrode M is the sum of the potential contributions V_A and V_B from the current source at A and the sink at point B.

$$V_M = V_A + V_B \tag{2.6}$$

From Equation 2.5:

$$V_M = \frac{\rho I}{2\pi}\left(\frac{1}{r_A} - \frac{1}{r_B}\right) \tag{2.7a}$$

Also, $V_N = \frac{\rho I}{2\pi}\left(\frac{1}{R_A} - \frac{1}{R_B}\right)$ (2.7b)

The potential difference (ΔV) between electrodes M and N is given as:

$$\Delta V = V_M - V_N = \frac{\rho I}{2\pi}\left\{\left(\frac{1}{r_A} - \frac{1}{r_B}\right) - \left(\frac{1}{R_A} - \frac{1}{R_B}\right)\right\} \tag{2.8}$$

$$\rho = \frac{2\pi\Delta V}{I\left\{\left(\frac{1}{r_A} - \frac{1}{r_B}\right) - \left(\frac{1}{R_A} - \frac{1}{R_B}\right)\right\}} \tag{2.9}$$

The geometric factor of any array, given as k, is written mathematically as:

$$k = \frac{2\pi}{\left\{\left(\frac{1}{r_A} - \frac{1}{r_B}\right) - \left(\frac{1}{R_A} - \frac{1}{R_B}\right)\right\}} \tag{2.10}$$

In some literature, it is written as:

$$k = \frac{2\pi}{\left\{\left(\frac{1}{r_1} - \frac{1}{r_2}\right) - \left(\frac{1}{r_3} - \frac{1}{r_4}\right)\right\}}$$

Where $r_1 = r_A$; $r_2 = r_B$; $r_3 = R_A$; and $r_4 = R_B$

Based on Ohm's law, a typical cylindrical wire carrying a current I, with length L (m), cross-sectional area A (m^2), and resistance R (Ω), has a measured resistance:

$$R = \frac{\Delta V}{I} \tag{2.11}$$

Hence, if Equations 2.10 and 2.11 are substituted in Equation 2.9, the apparent resistivity (ρ_a) is written as:

$$\rho_a = kR \tag{2.12}$$

ERM can generally be employed for several geophysical applications due to the wide range of ρ_a values for earth materials. The range of ρ_a values for some rocks, soils, and minerals are shown in Figure 2.2 and Table 2.1.

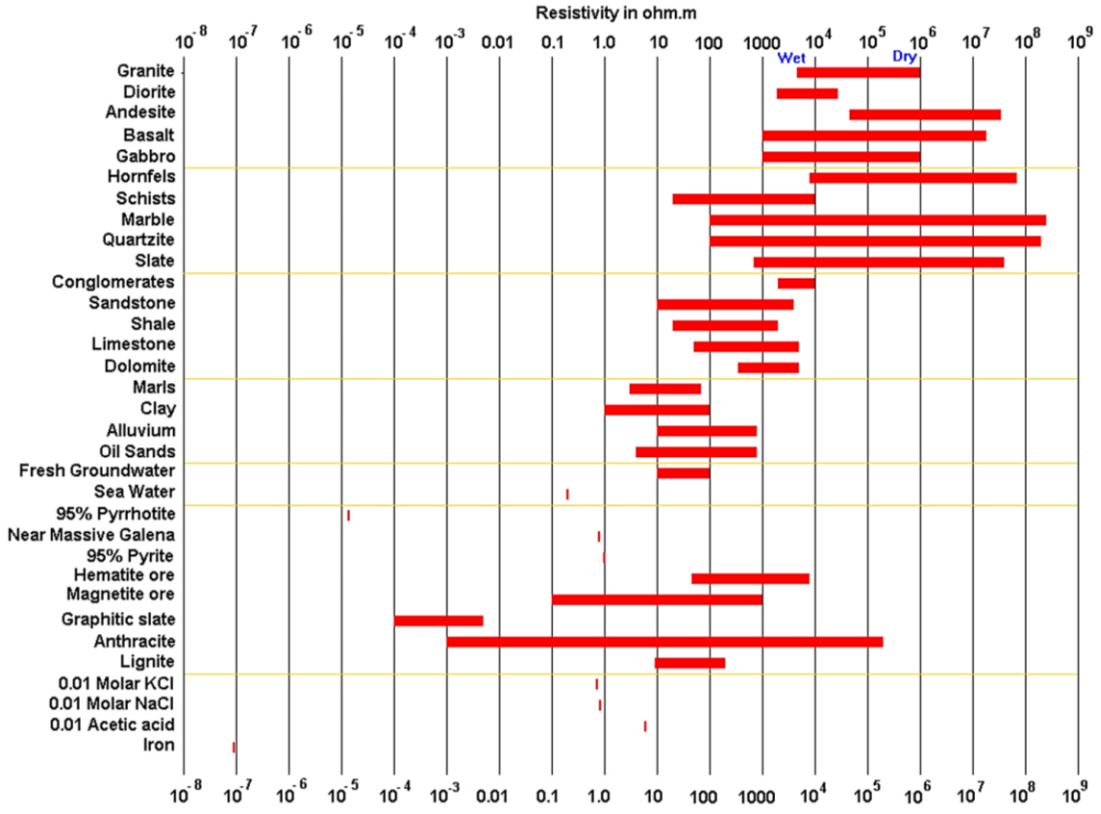

Figure 2.2 Resistivity chart for the range of values for rocks, soils, and minerals (after Telford et al., 1990).

Table 2.1 A comprehensive summary of the electrical resistivity values for some earth materials in different localities.

Common Materials	**Range of resistivity values (Ωm)**			
	Loke (2002)	Gibson & George (2013)	SEG (2014)	AGI (2008)
Clay	1 – 100	1 – 100	1 – 300	10 – 100
Sand	10 – 800	50 – 1050	1 – 1100	$600 - 1 \times 10^4$
Gravel	$600 - 10^4$	100 – 1400	20 – 7000	$600 - 1 \times 10^4$
Limestone	80 – 6000	$50 - 10^6$	----	$100 - 1 \times 10^6$
Shale	20 – 2000	----	3 – 200	----
Sandstone	10 – 5000	$1 - 7.4 \times 10^8$	10 – 700	$100 - 1 \times 10^3$
Granite	$5000 - 10^6$	$100 - 10^6$	300 – 40000	----

2.2.2 Configurations, Sensitivities, and Performance of Electrode Arrays

The electrical resistivity imaging electrodes have systematic arrangement modes known as array configuration. Only the spontaneous potential (SP) method has unique electrodes for its land and marine surveys. In practice, four electrodes (i.e., two current and two potential electrodes) are required for the electrical imaging or depth sounding. Electrodes may be placed on the ground surface, in boreholes, or at the surface/bottom of stream/river (via floating electrodes mechanism). A crucial element in reducing noise and enhancing the effectiveness and resolution of the method for identifying lateral and vertical structures is the choice of the selected electrode array configuration. For example in imaging, several electrode kinds, such as galvanized iron and aluminum electrodes, are noise-sensitive (LaBrecque & Daily, 2008). However, Daily et al. (2005) suggested that all electrodes are usable with any arrays, provided the survey lasts for a short time. An alternating power source is also used to avoid electrode polarization (Binley & Kemna, 2005).

Unlike the other electrodes, the copper electrode is easier to inject current into the ground because of its high conductivity that enables faster current flow. The electrode is resistant to corrosion but is rarely used due to its cost compared to other electrodes. On the other hand, the stainless steel electrode is often used for imaging and depth sounding due to its high sensitivity and relatively lower price. However, it has lower conductivity and is also vulnerable to corrosion than copper. Both electrodes may be sensitive to cultural/self-potential noise in the subsurface. Most importantly, electrodes' sensitivities and resolution capacities depend on electrode spacing, total spread length, amount of current introduced into the ground, depth of investigation, etc. A high-resolution tomographic model can be produced for a survey with small electrode spacing and short traverse due to shallow probing depth and ease of current penetration (Loke, 2002; Binley & Kemna, 2005; Daily et al., 2005; Loke et al., 2013; Binley, 2015; Binley et al., 2015; Mieszkowski et al., 2018; Akingboye & Ogunyele, 2019; Jiang et al., 2021; Akingboye et al., 2022).

There are several types of electrode arrays used for electrical investigations. The most commonly used arrays are Wenner, Schlumberger, Wenner-Schlumberger, dipole-dipole, pole-dipole, pole-pole, and gradient arrays. The uncommonly used ones are the optimized or modified arrays, which are products of the modifications of the commonly used arrays. These include the azimuthal square array, radial array, Cole-Cole array, Standard L and Corner array, Compare R and its noise-weighted array, etc. (Loke, 2002, 2004; Crook et al., 2008; Abdullah et al., 2018, 2019; Couto Junior et al., 2020). Some of these arrays employ two electrodes each for current and potential. Few use only one current and potential electrode, two currents and one potential electrode, or one current and two potential electrodes with the remaining current and potential electrodes spaced at an infinite distance (usually 20 times the normal electrode

separation). All these array configurations can image both lateral and vertical electrical variations, as well as detect 2-, 3- and 4-D anomalous bodies (Griffiths et al., 1990; Telford et al., 1990; Arora & Ahmed, 2011; Merritt, 2014; Binley et al., 2015; Bery et al., 2019; Hasan et al., 2020; Hojat et al., 2020; Rucker et al., 2021a; Szűcs et al., 2021).

Figure 2.3a–j shows the configurations, sensitivities, and performances of the electrode's quadrupole for some commonly used arrays. The schematic images depicting the lateral and vertical variations of subsurface electrical properties measured by these arrays are also provided. The Wenner array has three configuration types, namely the Wenner-Alpha (α), Wenner-Beta (β), and Wenner-Gamma (γ), with configurations of C1P1P2C2, C2C1P1P2, and C1P1C2P2, respectively (Figure 2.3a–c). Although the Wenner arrays have reduced horizontal sensitivity for sills and sedimentary structures, they are highly sensitive to detecting vertical changes below their centers (Loke et al., 2013; Merritt, 2014). As a result, the arrays may be best used in a noisy environment to derive appropriate vertical structures with high resolution (Loke, 2002). The Schlumberger array, with the same configuration C1P1P2C2, is similar to the Wenner- arrays but with closely spaced potential electrodes P1P2 (Figure 2.3d). The Schlumberger array's model coverage is narrower than the dipole-dipole array yet offers a slightly better horizontal resolution. This is because the closely spaced inner potential electrodes are sensitive to conditions around them (Loke, 2002; Merritt, 2014; Akingboye & Ogunyele, 2019).

The Wenner-Schlumberger array (Figure 2.3e) is a hybrid between the Wenner-alpha (α) array and the Schlumberger array (Pazdirek & Bláha, 2015; Balarabe et al., 2022). Wenner-Schlumberger has a greater median depth of

investigation, a weaker signal, and slightly wider horizontal data coverage than the Wenner array. The array, however, outperforms the dipole-dipole array in terms of signal power and narrower horizontal data coverage (Loke, 2002). This array is moderately sensitive to both horizontal and vertical structures. Thus, it is appropriate for deriving high-resolution models for both geological structures.

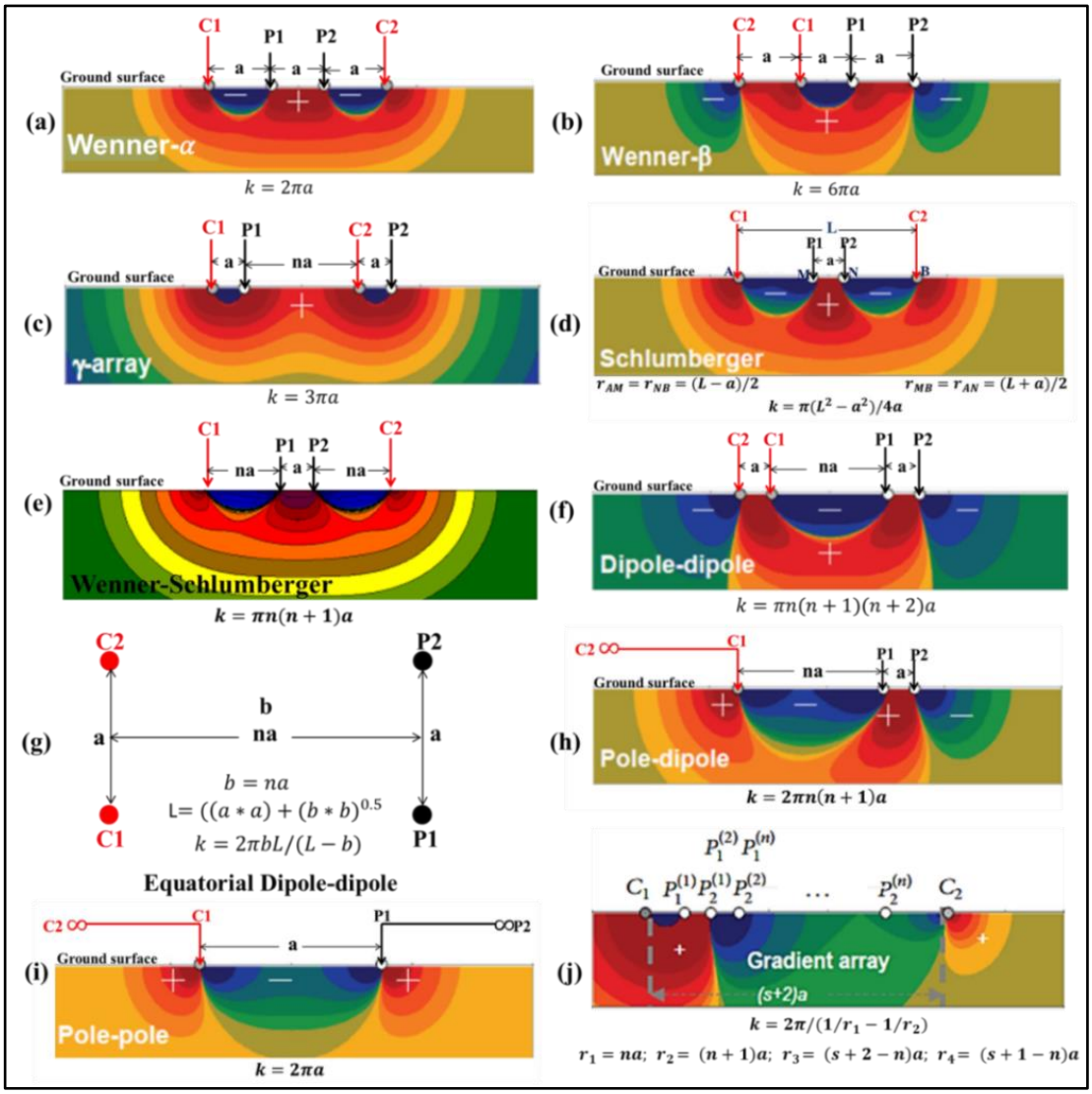

Figure 2.3 Array types with their respective geometric configurations of the electrode's quadrupole and geometric factors. C (1, 2) and P (1, 2) represent the current and potential electrodes, respectively. n is an integer value for dipole separation factor, a represents electrode spacing, k is the geometric factor, and ∞ implies infinity distance. The background inverted images show the performance and sensitivity patterns of the arrays. In the case of a gradient array, the first potential electrode pair $n\,factor = 1$ (modified after Akingboye & Ogunyele, 2019).